Photodissociation Dynamics of Nitromethane at 226 and 271 nm at Both Nanosecond and Femtosecond Time Scales

Y. Q. Guo, A. Bhattacharya, and E. R. Bernstein*

Department of Chemistry, Colorado State University, Fort Collins, Colorado 80523-1872

Received: July 15, 2008; Revised Manuscript Received: September 2, 2008

Photodissociation of nitromethane has been investigated for decades both theoretically and experimentally; however, as a whole picture, the dissociation dynamics for nitromethane are still not clear, although many different mechanisms have been proposed. To make a complete interpretation of these different mechanisms, photolysis of nitromethane at 226 and 271 nm under both collisional and collisionless conditions is investigated at nanosecond and femtosecond time scales. These two laser wavelengths correspond to the $\pi^* \leftarrow \pi$ and $\pi^* \leftarrow$ n excitations of nitromethane, respectively. In nanosecond 226 nm ($\pi^* \leftarrow \pi$) photolysis experiments, CH_3 and NO radicals are observed as major products employing resonance enhanced multiphoton ionization techniques and time-of-flight mass spectrometry. Additionally, OH and CH_3O radicals are weakly observed as dissociation products employing laser induced fluorescence spectroscopy; the CH_3O product is only observed under collisional conditions. In femtosecond 226 nm experiments, CH_3, NO_2, and NO products are observed. These results confirm that rupture of C−N bond should be the main primary process for the photolysis of nitromethane after the $\pi^* \leftarrow \pi$ excitation at 226 nm, and the NO_2 molecule should be the precursor of the observed NO product. Formation of the CH_3O radical after the recombination of CH_3 and NO_2 species under collisional conditions rules out a nitro−nitrite isomerization mechanism for the generation of CH_3O and NO from $\pi\pi^*$ CH_3NO_2. The OH radical formation for $\pi\pi^*$ CH_3NO_2 should be a minor dissociation channel because of the weak OH signal in both nanosecond and femtosecond (nonobservable) experiments. Single color femtosecond pump−probe experiments at 226 nm are also employed to monitor the dynamics of the dissociation of nitromethane after the $\pi^* \leftarrow \pi$ excitation. Because of the ultrafast dynamics of product formation at 226 nm, the pump−probe transients for the three dissociation products are measured as an autocorrelation of the laser pulse, indicating the dissociation of nitromethane in the $\pi\pi^*$ excited state is faster than the laser pulse duration (180 fs). In nanosecond 271 nm ($\pi^* \leftarrow$ n) photolysis experiments, pump−probe experiments are performed to detect potential dissociation products, such as CH_3, NO_2, CH_3O, and OH; however, none of them is observed. In femtosecond 271 nm laser experiments, the nitromethane parent ion is observed with major intensity, together with CH_3, NO_2, and NO fragment ions with only minor intensities. Pump−probe transients for both nitromethane parent and fragment ions at 271 nm excitation and 406.5 nm ionization display a fast exponential decay with a constant time of 36 fs, which we suggest to be the lifetime of the excited nπ^* state of nitromethane. Combined with the 271 nm nanosecond pump−probe experiments, in which none of the CH_3, NO_2, CH_3O, or OH fragment is observed, we suggest that all the fragment ions generated in 271 nm femtosecond laser experiments are derived from the parent ion, and dissociation of nitromethane from the nπ^* excited electronic state does not occur in a supersonic molecular beam under collisionless conditions.

I. Introduction

As a low sensitivity nitro-containing energetic material, nitromethane has been widely used in racing fuels, propellants, and explosives and has attracted a great deal attention because of its interesting physical and chemical properties. The absorption spectra and photochemistry of nitromethane have been studied extensively; however, the photodissociation dynamics of this simplest nitroalkane are still not clear due to the complication induced by its complex electronic structure. For the purposes of review, studies of the spectra and photochemistry of nitromethane are briefly summarized below.

The absorption spectrum of liquid phase nitromethane has been investigated in the early of 1900s[1−4] and is characterized by two regions of continuous absorption: a weak one with a maximum at about 300 nm and a strong one starting from 250 nm and extending toward shorter wavelength. Two decades later, Thompson and Purkis[5] revealed that the absorption of nitromethane in the gas phase starts from 304 nm and continues beyond 180 nm with a subsidiary minimum at 245 nm, which is in general agreement with Hirschlaff and Norrish's observations.[6] In the following years, the weaker absorption region was investigated extensively and found to peak near 276 nm.[7−9] More recently, Loos and co-workers'[10] showed that the absorption spectra of gas-phase nitromethane in the ultraviolet spectral region consist of two electronic bands: a strong band centered at 198 nm, which was first observed by Nagakura and assigned to a $\pi^* \leftarrow \pi$ transition localized on the NO_2 moiety,[11] and a much weaker band centered at 270 nm, which was assigned to a $\pi^* \leftarrow$ n transition from a nonbonding electron of O atom by Bayliss and McRae.[12] More information about other excited states are provided by electron impact spectra[13,14] and photoelectron spectra.[15]

* To whom correspondence should be addressed. Phone: 970-491-6347. Fax: 970-491-1801. E-mail: erb@lamar.colostate.edu.

10.1021/jp806230p CCC: $40.75
Published on Web 12/12/2008

In the early stages of the study of the decomposition of nitromethane, reaction 1 below has been suggested to be the primary process for the photolysis of nitromethane by Hirschlaff et al. [6] and Christie et al.[16]

$$CH_3NO_2 + h\nu \rightarrow CH_2O + NOH \quad (1)$$

Hirschlaff and Norrish performed a preliminary study of the decomposition of nitromethane in the gas phase using radiation of 300−200 nm. Their results show that the decomposition products can be interpreted quantitatively as resulting from reaction 1 followed by a secondary reaction of decomposition and oxidation by oximino (NOH) radicals. Christie and co-workers proposed that the same molecular elimination process is involved in the primary process of photolysis of nitromethane based upon the fact that the yield of formaldehyde is unaffected by the addition of nitric oxide.

Although Brown and Pimentel[17] have also observed the HNO radical as one of the primary products from the photolysis of nitromethane in solid argon at 20 K and 240−360 nm radiation, they suggest that the photolysis of nitromethane in matrix isolation proceeds in two steps

$$CH_3NO_2 + h\nu \rightarrow CH_3ONO \quad (2)$$

$$CH_3ONO + h\nu \rightarrow CH_2O + HNO \quad (3)$$

and that the nitro−nitrite isomerization is the primary process.

The nitro−nitrite isomerization process has been experimentally proved to be a competitive process with the rupture of C−N bond by Wodtke and co-workers[18] in their IR multiple photon dissociation studies of nitromethane.

To explain the high yield of nitrosomethane in their study of the photolysis of nitromethane in the liquid phase at 254 nm, Cundall and co-workers[19] suggest that an oxygen atom elimination process might be involved in the primary process

$$CH_3NO_2 + h\nu \rightarrow CH_3NO + O \quad (4)$$

Recently, Park and co-workers[20] have studied the dynamics of oxygen atom formation in the gas-phase photolysis of nitromethane using two UV photodissociation laser wavelengths, 248 and 266 nm, at room temperature. They concluded that at both photolysis wavelengths oxygen atoms are produced mainly via an indirect predissociation mechanism, but at 248 nm there is an additional contribution from a direct predissociation mechanism.

On the basis of the observation of OH radicals with a quantum yield of 0.004 under collision-free conditions, an OH formation dissociation pathway in the photolysis of nitromethane at 266 nm has been suggeted by Zabarnick et al.[21] Greenblatt et al.,[22] however, only observe the OH radical from photolysis of nitroalkanes with β- or γ-hydrogen through a five-membered ring intermediate at 282 nm. They did not detect any OH production from nitromethane.

Beyond the above different dissociation mechanisms, rupture of the C−N bond given by

$$CH_3NO_2 + h\nu \rightarrow CH_3 + NO_2 \quad (5)$$

under photolysis conditions is suggested as the main primary process of photolysis of nitromethane by several authors.[23−27] McGarvey and McGrath[28] and Napier and Norrish[29] have confirmed reaction 5 as the main primary process in the photodissociation process by observation of the strong absorption spectrum of the methyl radical immediately after flash photolysis (μs) of nitromethane. In both experiments, the formation of methyl nitrite is proposed to be a result of the recombination of methyl radical and nitrogen dioxide. Honda et al.[30] have determined the quantum yields of the main products methyl nitrite, formaldehyde, nitrosomethane, and NO from the photolysis of nitromethane in gas phase at 313 nm, 55 °C, and suggest that both reactions 1 and 5 are the primary processes of nitromethane photodecomposition based on the dependence of product quantum yields on the pressure of quenching gases. In addition, Bielski and Timmons[31] detected the ESR spectra of the methyl radical and nitrogen dioxide during photolysis of nitromethane at 77 K. Colles and co-workers[32] utilized opto-acoustic detection to provide the first spectral identification of the NO_2 fragment from continuous photolysis of nitromethane. Spear and Brugge[33] observed vibrationally excited NO_2 from photodissociation of nitromethane at 252.2 nm by laser-induced fluorescence.

The dynamics of the photodissociation of nitromethane after the excitation of the $\pi^* \leftarrow$ n transition near 270 nm in the picosecond time regime have been measured by Schoen et al.[34] and Mialocq et al.[35] Both groups observed ground state NO_2 fragments with high quantum yield within 5−6 ps after absorption of a single photon near 270 nm supporting their conclusion that excitation of the $\pi^* \leftarrow$ n transition near 270 nm results in dissociation predominantly via reaction 5. One exception is that, in a cross laser-molecular beam study of nitromethane, Kwok et al.[36] found that the excitation of nitromethane at 266 nm did not yield dissociation product under collision-free conditions.

Excitation of nitromethane in the $\pi^* \leftarrow \pi$ transition also gives reaction 5 as the primary process.[37−40] Blais[37] determined the dissociation cross section of nitromethane at 193 nm to be 1.7×10^{-17} cm^2 with near unity quantum yield. Butler et al.[38] have investigated the dissociation of nitromethane following the excitation of the $\pi^* \leftarrow \pi$ transition at 193 nm by product emission spectroscopy and molecular beam photofragment translational energy spectroscopy. For the first time they suggested that there are two distinct mechanisms by which the methyl radical and nitrogen dioxide are produced. The dominant mechanism produces vibrationally excited NO_2 in the first $^2B_2$ electronic state, much of which unimolecularly dissociates to NO and O atom. The minor mechanism produces NO_2 in a different excited state which could efficiently absorb a second 193 nm photon to further dissociate to NO and O atom. These mechanisms are further confirmed by Moss et al.[39] through observation of the production of two NO electronic states (X and A) and the appearance of two peaks in the translational energy distributions of CH_3 and O fragments from 193 nm photolysis of nitromethane. According to the polarized emission spectra from photodissociation of nitromethane excited at 200 and 218 nm, Lao et al.[40] suggested that the minor mechanism generates NO_2 in the second $^2B_2$ electronic state from the $^1B_2$ surface of nitromethane. A recent theoretical calculation showed, however, that the NO_2 from the major and minor channels should be assigned as (1^2B_1) and (1^2A_2), rather than (1^2B_2) and (2^2B_2).[41]

In a brief summary, inconsistencies still exist for the photodissociation mechanism of nitromethane, although it has been investigated for decades. NOH elimination, nitro−nitrite isomerization, O atom elimination, OH formation, and C−N bond rupture have all been suggested to be the primary process for the photodissociation of nitromethane under admittedly different experimental conditions, such as different phases, different temperatures, and different photodissociation wavelengths. Among these different mechanisms, the formation of NO_2 after C−N bond rupture has been the best accepted mechanism. The dynamics for the NO_2 formation following the

$\pi^* \leftarrow \pi$ excitation of nitromethane has not been measured to date, however. Although only two groups have tried to detect the OH radical from the photolysis of nitromethane, the final conclusions about OH radical formation are completely contrary: one group[21] did observe the OH radical with low quantum yield, while the other[22] did not. Moreover, several groups[34,35] observed NO_2 as a major dissociation product from photolysis of nitromethane after $\pi^* \leftarrow$ n excitation at relatively high pressure and room temperature. Kwok et al.[36] did not observe any dissociation product from the excitation of nitromethane at 266 nm under collision-free conditions. On the basis of these issues, we investigate the photodissociation of nitromethane at different wavelengths under different conditions so that we can compare our results with previous experiments to make as complete an interpretation as possible for the photodissociation of nitromethane at the nπ^* and $\pi\pi^*$ excited electronic states from an experimental point of view.

In this work, both nanosecond and femtosecond pump−probe techniques combined with time-of-flight mass spectrometry (TOFMS) and laser-induced fluorescence (LIF) spectroscopy are employed to study the dynamics of the photolysis of nitromethane at two laser wavelengths (226 and 271 nm), which correspond to the $\pi^* \leftarrow \pi$ and the $\pi^* \leftarrow$ n transitions of nitromethane, respectively. Photodissociation of nitromethane following $\pi^* \leftarrow \pi$ excitation has been investigated under both collisionless (in ionization/excitation region) and collisional (inside a quartz capillary) conditions. For comparison purposes, some experiments at 193 nm excitation have been repeated under similar experimental conditions as those for 226 nm excitation. In nanosecond 226 nm ($\pi^* \leftarrow \pi$ excitation) laser experiments, the NO, CH_3, and OH molecules are observed as dissociation products under both collisionless and collisional conditions, and the CH_3O species is only observed as a dissociation product under collisional conditions. Although the NO_2 product has not been directly observed in these experiments, we can still conclude that the C−N bond rupture should be the primary process of the photolysis of nitromethane at 226 nm based on the analysis of mass resolved excitation spectra (MRES) for the NO molecule and the direct observation of the CH_3 product. Moreover, the direct observations of CH_3, NO_2, and NO fragment ions without parent ion signal in femtosecond 226 nm excitation experiments further confirm that NO_2 elimination is the primary process of the photolysis of nitromethane at this wavelength. The observation of the OH radical with weak signal intensity in both nanosecond and femtosecond experiments indicates the OH radical formation should be a minor dissociation channel for nitromethane at 226 nm. Additionally, the observation of CH_3O species under collisional conditions rules out the nitro−nitrite isomerization mechanism but confirms that recombination of the CH_3 and NO_2 leading to the formation of methylnitrite does occur in the presence of collisions. The photodissociation dynamics of nitromethane at 226 nm excitation is determined to be faster than our laser pulse duration (180 fs). In nanosecond 271 nm ($\pi^* \leftarrow$ n excitation) laser experiments, pump−probe experiments are performed to detect potential dissociation products, such as CH_3, NO_2, CH_3O, and OH; however, none of them is observed. In femtosecond 271 nm laser experiments, the nitromethane parent ion is observed with major intensity, together with CH_3, NO_2, and NO fragment ions with only minor intensities. Pump−probe transients for both nitromethane parent and fragments ions at 271 nm excitation and 406.5 nm ionization display a fast exponential decay with a constant time of 36 fs, which we suggest to be the lifetime of the excited nπ^* state of nitromethane. Combined with the 271 nm nanosecond pump−probe experiments, in which none of the CH_3, NO_2, CH_3O, or OH fragment is observed, we suggest that all the fragment ions generated in 271 nm femtosecond laser experiments are derived from the parent ion and that dissociation of nitromethane from the nπ^* excited electronic state does not occur in a supersonic molecular beam under collisionless conditions.

II. Experimental Procedures

Detailed experimental procedures for nanosecond mass resolved excitation spectroscopy, LIF spectroscopy, and femtosecond laser pump−probe spectroscopy, have been described in our previous publications.[42−45] Briefly, the experimental setup consists of laser systems with both nanosecond and femtosecond time resolutions, a supersonic jet expansion nozzle, a TOFM spectrometer, and a LIF spectrometer. For the nanosecond laser experiments, the photolysis of the nitromethane at 226 nm excitation is performed at two different positions: one is in a quartz capillary attached to the supersonic jet expansion nozzle representing collisional conditions before molecular beam expansion; the other is in the ionization/excitation region of the spectrometers representing collisionless conditions after molecular beam expansion. The photolysis of nitromethane at 271 nm excitation is only performed in the ionization/excitation region under collisionless conditions.

In the 226 nm excitation experiments, a pump laser beam at 226 nm is used to initiate the dissociation of nitromethane and a probe beam with about 50 ns or 50 μs delay time depending on where the photolysis occurs are employed to detect photodissociation products. In the case for which both pump and probe beams are at the same wavelength (NO product detection) only a single beam is employed. The NO and CH_3 products are detected by one color resonance enhanced multiphoton ionization (REMPI) and TOFMS, through NO [$A\ ^2\Sigma^+ \leftarrow X\ ^2\Pi$] single photon and CH_3 [$4p\ ^2A'' \leftarrow X\ ^2A''$] two photon resonant transitions at 226 and 286 nm, respectively. The (0−0) and (0−1) rovibronic excitation spectra of fragment NO are obtained by scanning the laser wavelength around 226 and 236 nm, respectively. In addition, two other wavelengths at 303 and 308 nm are employed to probe CH_3O [$A\ ^2A_1 \leftarrow X\ ^2E, 2^1_0$] and OH [$A\ ^2\Sigma^+ (v'=0) \leftarrow X\ ^2\Pi (v''=0)$] species through LIF spectroscopy. In the nanosecond 271 nm experiments, the pump beam at 271 nm is used to excite the nitromethane molecule through the $\pi^* \leftarrow$ n transition, and a second beam at 532, 303, 286, or 308 nm is used to probe the potential NO_2, CH_3O, CH_3, or OH product.

The UV laser pulse used in the nanosecond laser experiments is generated by a pulsed dye laser, pumped by the second harmonic (532 nm) of a Nd:yttrium aluminum garnet laser's fundamental output (1.064 μm), in conjunction with a nonlinear wavelength extension system. To determine the dependence of the rotational temperature of fragment NO on the UV laser beam intensity, a 226 nm pulse energy of 16−300 μJ/pulse is used to provide laser beam intensities (I) of $\sim 6.5 \times 10^6$ to 1.2×10^8 W/cm^2 for an 8 ns pulse duration at a focused beam diameter of 0.2 mm. Up to 2 mJ energy of 271 nm has been used in the nanosecond LIF experiments. The pulse energy for different probe laser wavelengths varies from several hundreds of microjoule up to 5 mJ. Additionally, an excimer laser centered at 193 nm and a vacuum ultraviolet laser centered at 118 nm have also employed as pump and probe beams, respectively, to verify the fragments from photodissociation of nitromethane at 193 nm.

For femtosecond 226 nm pump−probe experiments, a single laser beam is equally split into pump and probe beams, and at

271 nm laser wavelength, the 271 nm beam is used as the pump pulse, and a second beam centered at 406.5 nm is used as the probe pulse. Sample molecules are excited by the pump beam and dissociate according to their dissociation dynamics. Dissociation products are subsequently ionized by the delayed probe beam and detected via TOFMS. By delaying the probe beam with respect to the pump beam, product appearance times can be determined. Three cases could be involved in the pump−probe transient analysis depending on different dynamic processes. First, if the dissociation dynamics are much slower than the laser pulse duration, the pump−probe transients for dissociation products should show a buildup then a plateau because of the relatively long lifetime of the fragments. In this case, we can extract the kinetic time employing a single exponential buildup function. Second, if the dissociation dynamics are much faster than the laser pulse duration, the pump beam can not only dissociate the sample molecule but can also ionize the dissociation products via nonresonance multiphoton ionization. In this case, rather than a buildup transient for the fragment, an autocorrelation (same frequency) or cross-correlation (different frequency) transient for the laser pulses would be observed, and an upper limit of the dynamic process can be determined to be faster than the laser pulse duration. Third, if sample molecule does not dissociate following excitation by the pump beam and the probe beam ionizes the sample molecule from its excited state, then the lifetime of the excited state of the sample molecule can be extracted from the pump−probe transient using single exponential decay function. Cases 2 and 3 are used to analyze the pump−probe transients following 226 and 271 nm excitation, respectively.

The femtosecond laser light is generated by a femtosecond laser system consisting of a self-mode-locked Ti:Sapphire oscillator (KM Laboratories), a homemade ring cavity Ti: Sapphire amplifier, and a commercial traveling wave optical parametric amplifier of super fluorescence (TOPAS, Light Conversion) system. The 226 nm laser pulse is the deep UV output from the TOPAS system which is pumped by the fundamental wavelength of 813 nm. Pulse duration of the deep UV laser pulse is measured to be 180 fs using a self-diffraction (SD) autocorrelator and off-resonance two-photon absorption of the furan molecule.[46] Typical pulse energy of the deep UV output is ~1 μJ/pulse. For one-color time-resolved investigations, the energy of pump and probe pulses is kept at an optimum value of ~200 nJ/pulse ($I \approx 5.66 \times 10^8$ W/cm^2) to improve signal-to-noise ratio and to avoid uncontrolled fragmentation due to multiphoton absorption by the parent molecule. The 406.5 and 271 nm laser beams, which are generated by two nonlinear β-BaB_2O_4 (BBO) crystals, are the second and third harmonics of the fundamental 813 nm femtosecond laser pulse. The energies of 406.5 and 271 nm laser pulses are about 15 and 2 μJ, respectively. The cross-correlation of the two beams is measured via the two photon nonresonance ionization of benzene molecule (as shown in Figure 1), which yields a time duration of the laser pulse of about 170 fs using the relation of $\tau_L = (1/2)^{1/2}$[full width at half maximum] (fwhm).

The experiment is run at a repetition rate of 10 Hz. The timing sequence for the pulsed nozzle, excitation laser, and ionization laser is controlled by a time delay generator (SRS DG535). The molecular beam is perpendicularly crossed by a UV laser beam that is focused to a spot size of about 0.2 mm at the ionization/excitation region of the spectrometer. A background pressure of 1×10^{-5} Torr is maintained in the vacuum chamber during the experiment. Ion signals are detected by a microchannel plate detector (MCP), and fluorescence signal is collected by a photomultiplier tube (PMT). Signals are recorded and processed on a personal computer using a box car averager (SRS SR 250) and an analog-to-digital conversion (ADC) card (Analog Devices RTI-800). For femtosecond time-resolved experiments, the delay time between the pump and probe beam is controlled by a microtranslation stage (Thorlabs: LNR50SEK1) with a step size of 13 fs. Each point on the pump−probe transient spectrum corresponds to an average intensity resulting from 100 laser shots.

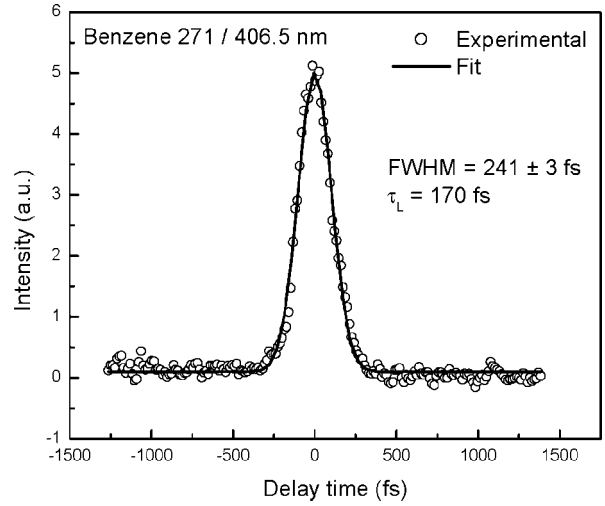

Figure 1. Measurement of femtosecond laser pulse cross-correlation between 271 nm (pump) and 406.5 nm (probe) wavelengths using off-resonance absorption of the benzene molecule. The laser pulse duration is determined to be 170 fs (τ_L = fwhm/$\sqrt{2}$).

A commercial nitromethane sample (Aldrich) is used in these experiments without additional purification. The vapor phase nitromethane molecules at room temperature are carried into the nozzle by helium carrier gas under a pressure of 30 psi through a glass vial. An NO_2 sample at a concentration of 0.01% is premixed with helium and 10% O_2, for use in spectrum comparison and system test.

III. Results and Discussion

A. Photodissociation of Nitromethane Following the $\pi^* \leftarrow \pi$ Excitation. Photolysis of nitromethane following the $\pi^* \leftarrow \pi$ excitation at 226 nm is investigated under both collisionless and collisional conditions. In both cases, the gas-phase nitromethane molecule is excited by absorbing a single 226 nm photon, which corresponds to the $\pi^* \leftarrow \pi$ strong absorption transition around 198 nm, and then dissociates into products along different dissociation pathways. The dissociation products after the $\pi^* \leftarrow \pi$ excitation are probed by either the same laser or a second time-delayed laser beam at different wavelength. To clarify which one of the possible dissociation channels of C−N bond rupture, OH formation, O atom elimination, or the nitro−nitrite isomerization is open at this electronic excitation, the CH_3, NO_2, NO, OH, CH_3O, and CH_3NO species have been probed by either TOFM or LIF spectroscopy. Since the 193 nm excitation of nitromethane belongs to the same $\pi^* \leftarrow \pi$ absorption transition, some of the experiments at this wavelength are repeated under similar conditions to those at 226 nm excitation, which leads to a close comparison between these two wavelengths for the same absorption excitation. The results for each possible dissociation mechanism are presented and discussed in following subsections.

1. Observation of CH_3, NO, and NO_2 Fragments. The primary fragmentation products after the $\pi^* \leftarrow \pi$ excitation of

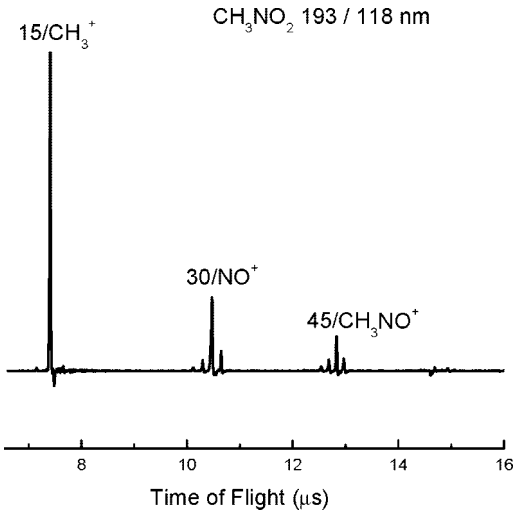

Figure 2. Mass spectrum of the photodissociation of nitromethane following excitation of $\pi^* \leftarrow \pi$ transition using 193 nm nanosecond laser pulses. A nanosecond 118 nm laser pulse is employed to ionize the dissociation products. CH_3, NO, and CH_3NO are apparent product peaks; small peaks around NO and CH_3NO are impurity signals from 193 nm ionization.

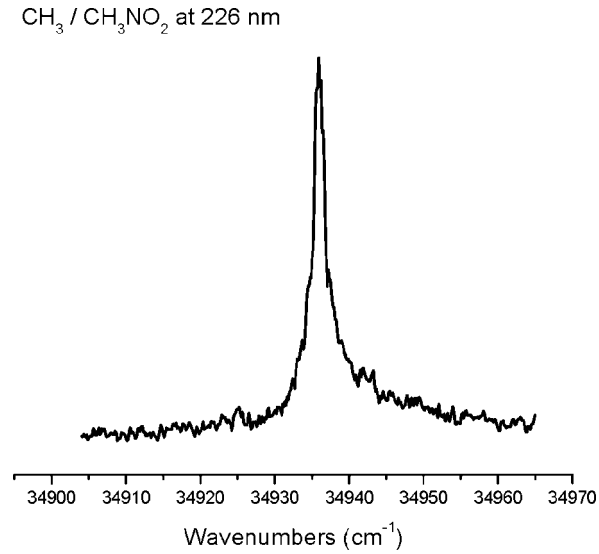

Figure 3. One-color (286 nm), two-photon resonance enhanced ionization MRES of the CH_3 [4p $^2A'' \leftarrow X\ ^2A''$] product from photolysis of nitromethane at 226 nm.

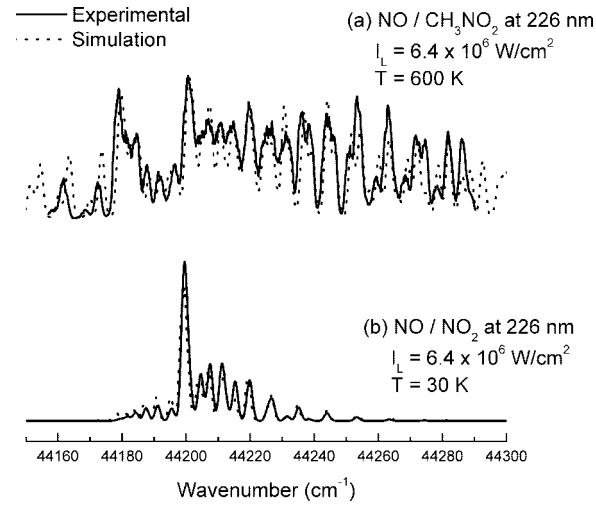

Figure 4. One-color (226 nm) MRES of the NO [A $^2\Sigma^+$ ($v' = 0$) $\leftarrow$ X $^2\Pi$ ($v'' = 0$)] product from photolysis of nitromethane (a) and NO_2 (b) at 226 nm. The solid lines are experimental measurements; the dotted lines are simulations by Boltzman population distribution, which produce rotational temperatures of 600 and 30 K for the NO product from nitromethane and NO_2, respectively, at a laser intensity of 6.4×10^6 W/cm^2.

nitromethane are suggested to be CH_3 and NO_2.[38] The NO_2 fragment in the 1^2B_2 excited state can automatically dissociate into NO (X) and O (^3P) as secondary products when the excitation photon energy is high enough. As illustrated in the mass spectrum (Figure 2) obtained by 193 nm excitation of nitromethane in the ionization region of the TOFM spectrometer employing 118 nm ionization of dissociation products, the CH_3 mass channel shows an intensity of about 4.5 times that of the NO mass channel, produced from the dissociation of the NO_2 fragment. This confirms that the C−N bond rupture is the main primary process for the dissociation of nitromethane following the $\pi^* \leftarrow \pi$ excitation and that the NO_2 molecule should be the precursor for the NO product. The third peak (mass channel 45 amu) is given by O atom elimination from nitromethane and will be discussed later. Several other weak peaks around the three major peaks are impurity signals derived from 193 nm ionization.

For 226 nm excitation of nitromethane in the ionization region, the 118 nm ionization detection scheme can not probe the dissociation products due to the low energy of both 226 and 118 nm laser pulses. Therefore, one color REMPI is employed to probe both CH_3 and NO products from the photolysis of nitromethane at this wavelength (226 nm). The MRES spectrum of CH_3 radical is presented in Figure 3. This spectrum is generated by one color (286 nm), two photon, resonance absorption from the CH_3 ground electronic state to its 4p Rydberg state [4p $^2A'' \leftarrow X\ ^2A''$], and a third photon is required to ionize the CH_3 radical from the excited state to CH_3^+. The only distinguishable feature in this spectrum is a very strong, sharp Q branch with no resolved rotational structure. The rotational temperature of CH_3 radical has been determined to be 200 K with large uncertainty by Moss and co-workers in their 193 nm excitation experiment.[39] This confirms that the CH_3 product from $\pi\pi^*$ excited state decomposition of nitromethane is relatively rotationally cold. The NO product in its ground electronic state is probed at the same wavelength (226 nm) through its $A^2\Sigma^+$ ($v' = 0$) $\leftarrow X^2\Pi$ ($v'' = 0$) transition. Figure 4a shows a one-color MRES spectrum of the NO product from photodissociation of nitromethane at 226 nm. The spectrum is rotationally resolved, and most of the recorded features belong to the $^2\Pi_{1/2}$ component of the ground electronic state. The most intense feature in this spectrum can be assigned as the ($Q_{11} + P_{12}$) band head of the (0−0) vibronic band, and the less intense features are due to other rovibronic transitions.[47,48] Spectral simulation based on the Boltzman population distribution produces a rotational temperature of 600 K for the NO product under the laser intensity used for recording this spectrum. In addition to the (0−0) vibronic band, the (0−1) vibronic band is also observed with similar rotational distribution. The hot rotational distribution of NO product from photodissociation of nitromethane after the $\pi^* \leftarrow \pi$ excitation at 226 nm is in good agreement with Moss et al.'s observation,[39] from which they determined the rotational temperature of the NO product from 193 nm photolysis of nitromethane to be 1000 K.

According to the energy level diagram for photodissociation of nitromethane following the $\pi^* \leftarrow \pi$ excitation,[39] however, a single 193 nm photon (6.4 eV) has enough energy to produce

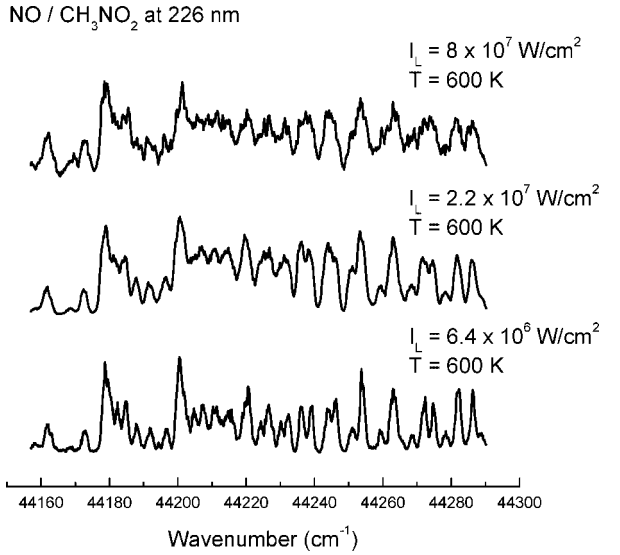

Figure 5. Comparison of the one-color MRES of the NO [A $^2\Sigma^+$ (v′ = 0) ← X $^2\Pi$ (v″ = 0)] product from photolysis of nitromethane at different intensities of 226 nm laser pulses.

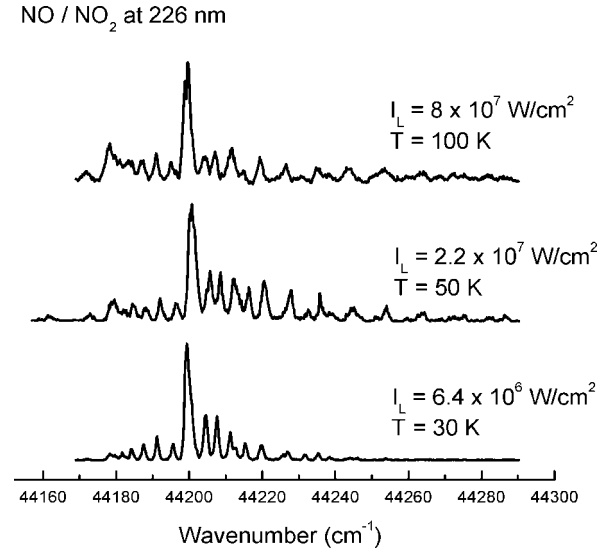

Figure 6. Comparison of the one-color MRES of the NO [A $^2\Sigma^+$ (v′ = 0) ← X $^2\Pi$ (v″ = 0)] product from the photolysis of NO_2 at different intensities of 226 nm laser pulses.

the NO product in its ground electronic state through an excited NO_2 intermediate. This process needs at least 5.8 eV energy, but a single 226 nm photon (5.5 eV) has only enough energy to produce an excited NO_2 (1^2B_2) molecule, which does not have enough internal excitation energy to decompose further into an NO product. Therefore, the NO_2 product in its 1^2B_2 excited state needs to absorb a second photon from the 226 nm excitation laser to be dissociated into an NO product, which displays relatively higher vibrational temperature (both v″ = 0 and 1 are observed) and lower rotational temperature (600 K) than the NO from 193 nm excitation, for which only v″ = 0 is observed, and the rotational temperature is about 1000 K.

For comparison purposes, the MRES spectrum of the NO product from photodissociation of NO_2 molecule at 226 nm is presented in Figure 4b. Both spectra are obtained under similar low laser intensity. A single 226 nm photon excites NO_2 to its 2^2B_2 state[49] with high vibrational excitation. The excited NO_2 molecule then dissociates into an NO in its ground electronic state and O in its ^1D excited state.[50] The NO product from this NO_2 excited state (2^2B_2) shows a rotational distribution of about 30 K, much colder than the NO product from the NO_2 (1^2B_2) produced in the photolysis of nitromethane. Since the NO_2 molecule from both the dissociation of nitromethane at 226 nm and the NO_2 gas sample must absorb one 226 nm photon to dissociate into an NO product, based on the large rotational temperature difference of the NO product, one can conclude that the NO_2 product from the dissociation of nitromethane is not in its ground electronic state. The ground state NO_2 product is also probed by LIF spectroscopy through 532 nm excitation after the dissociation of nitromethane at 226 nm. No fluorescence signal is observed from the NO_2 molecule, which further confirms that most of the NO_2 products generated from nitromethane are in the excited electronic state (1^2B_2).

The spectra of the NO product from photolysis of nitromethane probed at different laser (226 nm) intensities are shown in Figure 5. Except for the distortion due to power broadening, all spectra show a similar pattern, which produces about the same rotational temperature of 600 K for the NO product. Thus we conclude that the rotational temperature of the NO product from photodissociation of nitromethane at 226 nm excitation is laser intensity independent. Similar spectra of the NO product from photodissociation of NO_2 with different laser beam intensities are shown in Figure 6, in which one can find that the rotational temperature of the NO product from NO_2 molecule is laser intensity dependent. At the maximum laser intensity used in these experiments, a rotational temperature of about 100 K is observed, much hotter compared to the NO product produced at low laser intensity, which is about 30 K.

At high laser intensity, NO production from the dissociation of NO_2 at 226 nm has been fully investigated.[51] The conclusion is that four-photon absorption process can occur for the fragmentation of NO_2 and the excitation and ionization of NO product at high laser intensity. Two photons excite the NO_2 molecule, and another two excite and ionize the NO (X) product. Two possible excited states of the NO_2 have been suggested as candidates for the NO_2 dissociative states after absorption of two photons at 226 nm: a Rydberg state at 10.85 eV and an ion-pair state. For either state, the dissociation dynamics can produce an NO(X) predominantly with hot rotational and vibrational energy distributions. Since two different pathways are involved in the dissociation of NO_2 molecule at high laser intensity, the rotational distribution of the NO product at different laser intensity should be the superposition of the NO product from both dissociation pathways, which results in different rotational temperatures of the NO product at different laser intensities.

Although two different channels for the production of NO_2 in two different excited state (1^2B_2 and 2^2B_2) have been proposed in the dissociation of nitromethane at 193 nm,[38,40] only the major channel which produces NO_2 in 1^2B_2 state is open at 226 nm excitation because the $CH_3 + NO_2$ (2^2B_2) dissociation limit is about 19 kcal/mol higher than the photon energy of 226 nm wavelength. As mentioned above, the NO_2 (1^2B_2) from the 226 nm photodissociation of nitromeathane absorbs a second photon and then dissociates into an NO ($X^2\Pi$) product with hot rotational and vibrational distributions. This is different from the NO_2 (2^2B_2) prepared by absorption of a 226 nm photon by NO_2 gas, which is highly vibrationally excited and can dissociate into NO (X) with cold rotational and vibrational distributions. Under high laser intensity irradiation, the NO_2 (2^2B_2) can easily absorb a second 226 nm photon and reach a Rydberg or ion pair state and then dissociates into NO (X) with a hot rotational distribution through a different channel. This could be a

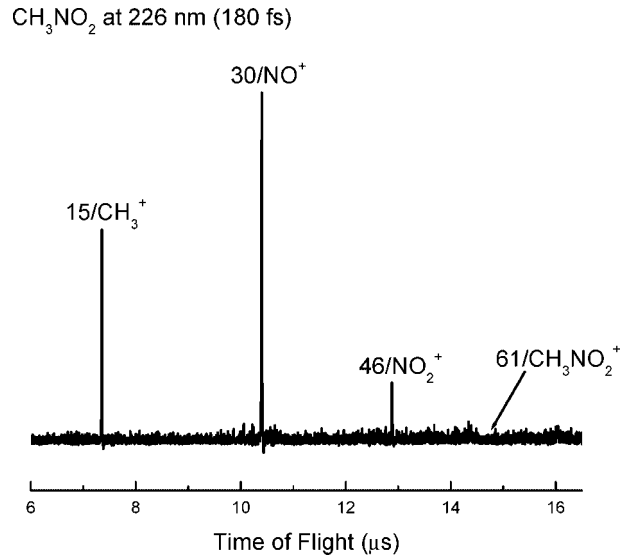

Figure 7. Mass spectrum of the photolysis of nitromethane following $\pi^* \leftarrow \pi$ excitation at femtosecond 226 nm. The parent ion at mass channel 61 amu is not observed.

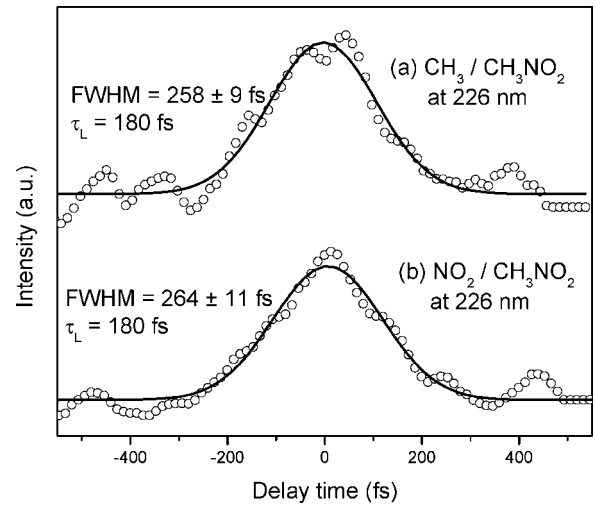

Figure 8. Femtosecond pump−probe transients for the CH_3 (a) and NO (b) fragments from the photolysis of nitromethane at 226 nm. Open circles are experimental measurements; solid lines are Gaussian fittings. Both transients show an autocorrelation of laser pulses with time duration of about 180 fs.

reasonable explanation for the different laser intensity dependence of the dissociation of nitromethane and NO_2 via 226 nm excitation. Moreover, the laser intensity independence of the NO product from nitromethane further confirms that the NO_2 product is not in its ground electronic state.

The TOFM spectrum of the photodissociation of nitromethane under femtosecond 226 nm irradiation is presented in Figure 7. Three major mass channels with mass of 15, 30, and 46 amu, corresponding to CH_3, NO, and NO_2 ions are observed after the photodissociation of nitromethane at this wavelength. Nitromethane parent ion is not observed. The line width for these three fragment mass peaks varies from 10 to 13 ns, which is the instrumental line width of the TOFMS spectrometer. Since the CH_3, NO_2, and NO radicals are directly observed as photodissociation products from nitromethane following nanosecond 226 nm excitation and the line width for the three fragment mass peaks is not broadened, we can conclude that the fragment ion signal is not from the fragmentation of nitromethane parent ion (not observed) but rather from the ionization of neutral dissociation products following $\pi^* \leftarrow \pi$ excitation. The direct observation of CH_3 and NO_2 fragments further confirms that rupture of C−N bond should be the primary process for the photolysis of nitromethane after the excitation of $\pi^* \leftarrow \pi$ transition. NO is a secondary product from the unimolecular dissociation of the NO_2 fragment.

An explanation based on orbital grounds for the C−N bond dissociation pathway following $\pi^* \leftarrow \pi$ excitation of nitromethane, assigned to the $1^1B_2 \leftarrow X$ transition, has been given by Lao et al.[40] On the basis of analysis of nitromethane orbital symmetry and NO_2 molecule electronic transitions, they point out that the 1^1B_2 excited electronic state of nitromethane correlates diabatically to the $CH_3 + NO_2$ (2^2B_2) dissociation limit. Additionally, if the 1^1B_2 excited electronic state were predissociated by a repulsive $^1B_2$ ($n\sigma^*$) electronic state as suggested by Mijoule et al.,[52] then the adiabatic dissociation pathway following excitation to the 1^1B_2 excited electronic state would produce $CH_3 + NO_2$ (1^2B_2).

To measure the dynamics of the formation of CH_3 and NO_2 fragments, a single 226 nm femtosecond beam is equally split into pump and probe beams with identical intensity. The nitromethane molecule is pumped to its excited state by absorbing a single photon from the pump beam and then dissociates into CH_3 and NO_2 products. The products are further excited and ionized by absorbing one or two photons from the probe beam. By scanning the delay time between the pump and probe beams, we should obtain transients illustrating the exponential buildup time of the fragments if the dissociation dynamics of nitromethane is much slower compared to the time duration of our laser pulse. On the other hand, if the dynamics of the dissociation of nitromethane is much faster than the laser pulse duration, the pump beam can not only fragment the parent molecule but also excite and ionize the fragments by nonresonant two-photon absorption. In this case, we will not observe the buildup of the fragments but an autocorrelation between the pump and probe beams near the zero delay time. The pump−probe transients for the fragments CH_3 and NO_2 from the dissociation of nitromethane are shown in parts a and b of Figure 8. Rather than an exponential buildup transient for the fragments, both parts a and b of Figure 8 present autocorrelation curves which can be fitted by a Gaussian pulse shape with time duration of 180 fs. Thus we conclude that the photodissociation of nitromethane at 226 nm in femtosecond time regime is faster than our laser pulse duration. To date, no direct dynamics measurement of the photodissociation of nitromethane following the $\pi^* \leftarrow \pi$ excitation has been reported.

2. Observation of CH_3NO. In Figure 2, in addition to the CH_3 and NO products from the C−N bond rupture pathway, a third product CH_3NO with mass of 45 amu shows that O atom elimination also occurs after the $\pi^* \leftarrow \pi$ excitation of nitromethane. Compared to the signal intensity of CH_3 and NO products, the CH_3NO product displays relatively weak intensity, especially since some impurity signal is also present at this mass channel. The direct observation of a CH_3NO peak with weak intensity confirms that the O atom elimination should be one of the dissociation pathways for nitromethane following the $\pi^* \leftarrow \pi$ excitation with a small branching ratio. This observation is consistent with Park and co-workers' studies of photolysis of nitromethane at 248 nm, in which they observed some O atom intensity contributed from a direct predissociation mechanism.[20] Both Park's and our observations are different from Cundall and co-workers' results that a high yield formation of nitrosomethane is obtained from photolysis of nitromethane in liquid at 254 nm. The possible reason for the difference might

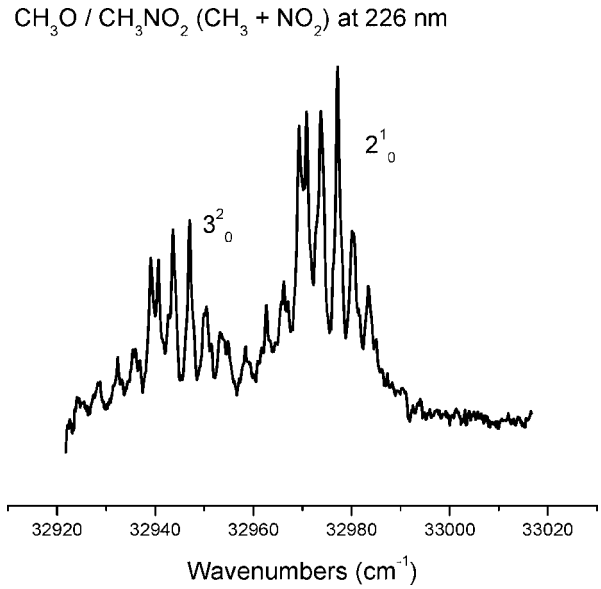

Figure 9. The LIF spectrum of CH_3O [A $^2A_1 \leftarrow$ X ^2E] product derived from recombination of CH_3 and NO_2 products from the photolysis of nitromethane at 226 nm in a quartz capillary (collisional conditions).

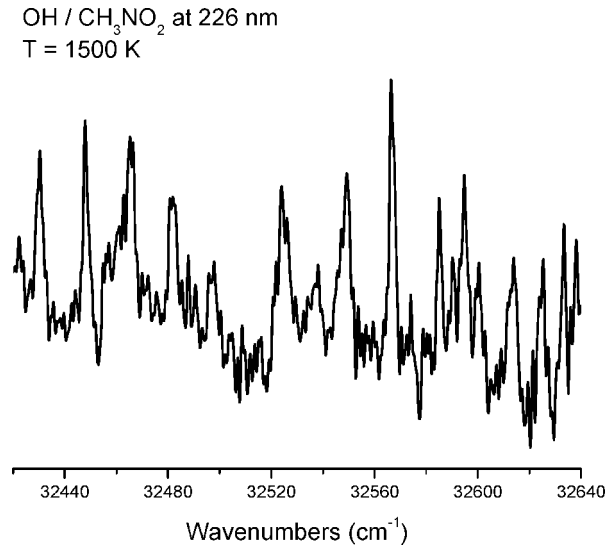

Figure 10. A portion of the LIF spectrum of OH [A $^2\Sigma^+$ (v′ = 0) ← X $^2\Pi$ (v″ = 0)] product from the photolysis of nitromethane at 226 nm. The OH product has a 1500 K rotational population distribution.

be that intermolecular interactions of the excited nitromethane molecule in liquid play a role in the formation of nitrosomethane. Moreover, different wavelength excitations could also lead to different primary dissociation processes.

3. Observation of CH_3O Radical. The nitro−nitrite isomerization mechanism has been determined to be the primary process by Brown and Pimentel in their photolysis of nitromethane in solid argon at 20 K and 240−360 nm radiation.[17] Additionally, Wodtke and co-workers observed that the nitro−nitrite isomerization is competitive with the rupture of C−N bond in their IR multiphoton dissociation studies of nitromethane.[18] On the contrary, several groups suggested that the methyl nitrite should be a result of the recombination of CH_3 radical and NO_2.[28,29] To confirm that the nitro−nitrite isomerization is one of the dissociation pathways for nitromethane following $\pi^* \leftarrow \pi$ excitation, the CH_3O radical is probed by LIF spectroscopy after the excitation of nitromethane at 226 and 193 nm in both the excitation region of the LIF spectrometer and in the quartz capillary attached to the supersonic jet expansion nozzle. The fluorescence signal of the CH_3O product after the A $^2A_1 \leftarrow$ X ^2E excitation can only be observed under collisional conditions when the photolysis of nitromethane is performed inside the quartz capillary. The excitation fluorescence spectrum of the CH_3O radical is illustrated in Figure 9 for two transition bands (3_0^2 and 2_0^1) along with their rotational structures. No CH_3O radical signal is observed under collisionless conditions, but a relatively intense signal is observed for CH_3O under collisional conditions. Thus, formation of CH_3O is not directly by way of a nitro−nitrite isomerization mechanism but as a result of recombination of the CH_3 and NO_2 species after the C−N bond rupture. This is in good agreement with McGarvey[28] and Napier's[29] suggestion. It also confirms that the NO product observed in the ionization/excitation region of the TOFM and LIF spectrometers is not from the isomerization intermediate (CH_3ONO) but from the secondary dissociation of NO_2 product. In addition, since Wodtke and co-workers observed the nitro−nitrite isomerization product from their IR multiphoton dissociation of nitromethane in its ground electronic state, we may infer that the nitro−nitrite isomerization mechanism takes place in the dissociation of nitromethane from the ground electronic state, but not from its excited electronic states (at least $\pi\pi^*$ thus far).

4. Observation of OH Radical. In gas-phase photolysis of nitromethane, two groups tried to detect the OH radical as a dissociation product. Zabarnick and co-workers observed the OH radical with a quantum yield of 0.004 from photolysis of nitromethane at 266 nm;[21] however, Greenblatt and co-workers did not observe the OH radical from their photolysis of nitromethane at 282 nm.[22] The mechanism for the OH radical formation is not clear yet, although Zabarnick pointed out that OH is generated via a mechanism not involving a five-membered ring formation. Thus, we search for an OH product by LIF spectroscopy following 226 nm excitation of nitromethane in both the excitation region of the LIF chamber (no collisions) and the quartz capillary attached to the nozzle (collisions). In the excitation region of the LIF spectrometer, a very weak fluorescence signal (a few millivolts) is observed by a 308 nm probe laser through the OH [A $^2\Sigma^+$ (v′ = 0) ← X $^2\Pi$ (v″ = 0)] transition. The fluorescence excitation spectrum of OH is presented in Figure 10, characterized by a very hot rotational spectral structure. Simulations based on a Boltzman population distribution give a rotational temperature for OH X $^2\Pi$ (v″ = 0) of 1500 K. The OH radical is also observed with relatively stronger intensity but much colder rotational distribution (30 K) after the photodissociation of nitromethane in the quartz capillary. Supersonic expansion following formation of the OH radical inside the quartz capillary cools down the dissociation product (OH), and leads to the band head spectral line intensity increasing. At 193 nm excitation, in both the LIF excitation region and quartz capillary, the OH radical is also observed as a photodissociation product with similar rotational distribution to that at 226 nm excitation. The Franck−Condon factor for the (0−1) vibronic band of the OH radical is about ten time less than that of (0−0) band, based on the weak intensity of the (0−0) vibronic band, we do not expect to observe the (0−1) vibronic band of the OH radical transition in our experiments.

Since Greenblatt et al.[22] have only observed OH formation from dissociation of nitroalkanes with β- or γ-hydrogen, such as nitroethane, nitropropane, and nitrobutane, but not from dissociation of nitromethane at 282 nm, one must consider the possibility that the OH formation observed in our experiment

is not from dissociation of $\pi\pi^*$ nitromethane but from dissociation of larger nitroalkane impurities in the nitromethane sample. GC-MS analysis shows that the only nitroalkane impurity in the nitromethane sample used in our experiment is nitropropane of <0.1%. To confirm that the OH signal observed in our experiments is not generated from dissociation of nitropropane, we have compared OH formation from photodissociation of HNO_3 to that from nitromethane at 193 nm excitation to estimate the quantum yield for OH formation from nitromethane dissociation. Under roughly the same experimental conditions, such as laser intensity, concentration, and so on, we obtain a ratio of 1:25 for the OH signal intensity from dissociation of nitromethane and HNO_3 at 193 nm. The absorption cross sections for nitromethane[37] and HNO_3[53] at 193 nm are 1.7×10^{-17} and 1.2×10^{-17} cm^2, respectively, and the OH formation quantum yield for HNO_3 at this wavelength is about 0.93.[54] Thus we can obtain an approximate OH formation quantum yield of 0.03 for nitromethane dissociation at 193 nm. By assumption that the quantum yield for OH formation from nitropropane dissociation has about the same value, the OH signal intensity will be about 2000 times lower than what we have observed because the concentration and vapor pressure of nitropropane are about 1000 and 2.2 times, respectively, less than that of nitromethane. Therefore the OH signal must be generated from the dissociation of nitromethane following the $\pi^* \leftarrow \pi$ excitation.

The mechanism for the OH radical formation from photolysis of nitromethane is not clear to date. Since the NO product is observed as a dissociation product above, it is very possible that both the NO and OH radicals are generated from an HONO intermediate formed through a five- or four-membered ring mechanism. To form a five-membered ring in a nitromethane molecule, nitro−nitrite isomerization should occur first. The nitro−nitrite isomerization mechanism is ruled out by the observation of CH_3O product under only collisional conditions, however. Therefore, if the OH radical is generated from secondary dissociation of HONO intermediate, the dissociation of nitromethane in the $\pi\pi^*$ excited electronic state should involve a four-membered ring formation mechanism. To ensure that the NO product is not mostly from the secondary dissociation of an HONO intermediate, we also measured the NO fluorescence signal after the 226 nm excitation of nitromethane. The maximum signal intensity of NO fluorescence is about 1 V, and the LIF excitation spectrum of NO product shows a rotational temperature of about 600 K, which is similar to the MRES spectrum of the NO product. On the basis of the analysis of Franck−Condon factors and Boltzman population distributions of NO and OH species, the signal intensity ratio between NO and OH radicals should be about 1:3 assuming both are derived from the same precursor. The signal intensity of NO is much greater than that of OH, and therefore we conclude that HONO formation is at most a minor channel for the photodissociation of nitromethane following $\pi^* \leftarrow \pi$ excitation, and the NO product is mostly derived from the secondary dissociation of the primary NO_2 product.

As discussed above, O atom elimination does occur following the $\pi^* \leftarrow \pi$ excitation of nitromethane. Thus, we can not rule out the formation of an OH radical through H atom extraction from methyl group of any possible dissociation products (such as CH_3, CH_3NO, or even nitromethane) by O atom.

B. Photodissociation of Nitromethane Following the $\pi^* \leftarrow$ n Excitation. Since both Shoen et al.[34] and Mialocq et al.[35] have reported ground state NO_2 as a major photodissociation product following $\pi^* \leftarrow$ n excitation of nitromethane by picosecond excitation at 266 nm at room temperature, nanosecond laser pump−probe experiments are carried out to detect the NO_2 product from photolysis of nitromethane at 271nm excitation. A 532 nm laser beam is used as the probe beam, and the fluorescence signal from NO_2 gas after 532 nm excitation is shown in Figure 11 under collisionless conditions. After a careful search for the NO_2 fluorescence signal following $\pi^* \leftarrow$ n excitation of nitromethane in the supersonic molecular beam at 271 nm, we did not observe any fluorescence signal through a pump−probe, collisionless detection scheme. This observation shows that NO_2 product is not generated at 271 nm excitation of nitromethane in the supersonic molecular beam under collisionless conditions. Compared with Shoen and Mialoq's experimental conditions, the observation of the ground state NO_2 production in their experiments might be ascribed to high pressure and high temperature.

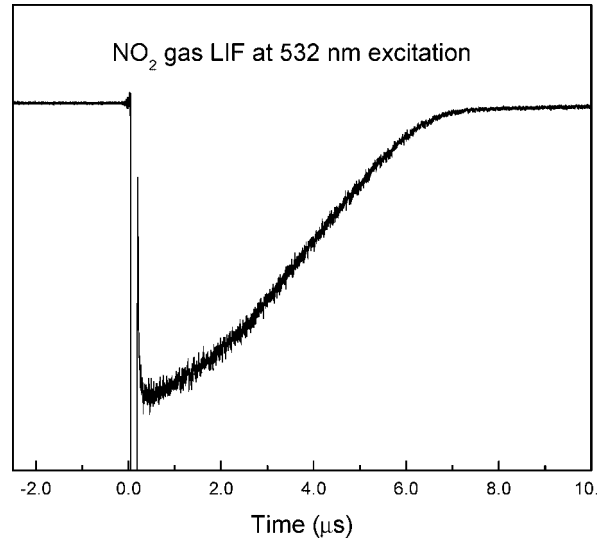

Figure 11. Fluorescence signal from excited NO_2 molecule at 532 nm excitation of NO_2 gas.

As mentioned above, the OH radical has been detected as a product through a minor dissociation channel for nitromethane following $\pi^* \leftarrow \pi$ (226 nm) excitation. Therefore, we perform similar pump−probe experiments at 271 nm excitation of nitromethane to probe the generation of OH radicals. Under the detection sensitivity limit of our LIF spectrometer for OH species, no OH radical fluorescence signal is observed. This observation is in good agreement with Greenbaltt and coworkers' study,[22] in which they did not observe any OH production from photolysis of nitromethane at 282 nm.

Attempts are also made to detect the CH_3 and CH_3O radicals following the 271 nm excitation of nitromethane under collisionless conditions, but no signal for either CH_3 or CH_3O is observed.

Figure 12 shows the TOFMS of the photolysis of nitromethane at femtosecond 271 nm excitation. Three fragment ions (CH_3, NO_2, and NO) are observed with only minor intensities, and the nitromethane parent ion is observed with major intensity. The minor fragment ion signal intensity could be explained in two different ways: one is that most of the excited parent molecules are ionized by absorption of another two photons at 271 nm, and only a very small portion of the excited molecules dissociates into CH_3 and NO_2 after rupture of C−N bond. After the dissociation occurs, the fragments can be further ionized by absorption of another three photons at 271 nm. We call this a dissociation−ionization mechanism. In this case, the line width for the parent ion mass peak and fragment ion mass peaks should be about the same (10 ns), and no broadening should occur to

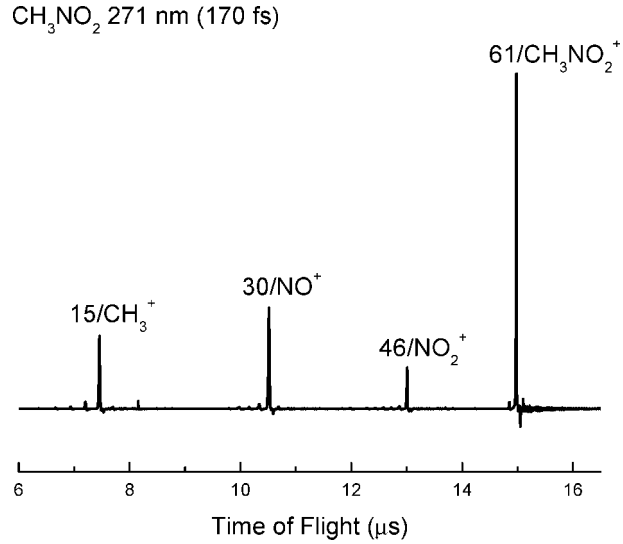

Figure 12. Mass spectrum of the photolysis of nitromethane following $\pi^* \leftarrow$ n excitation at femtosecond 271 nm. Intense parent ion signal at mass channel 61 amu is observed.

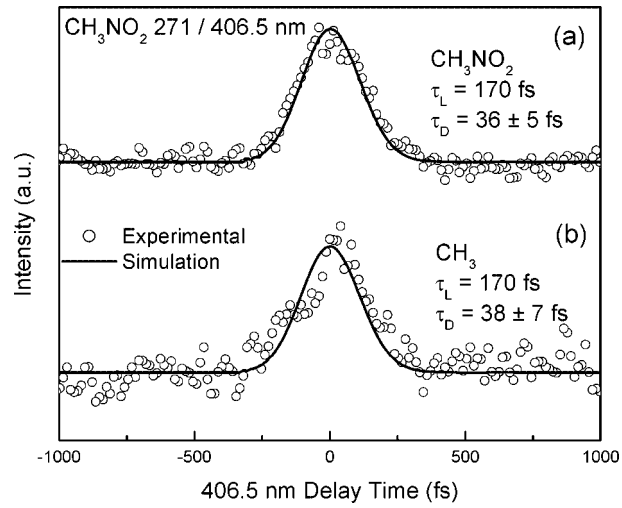

Figure 13. Femtosecond pump−probe transients for the nitromethane parent (a) and CH_3 fragments (b) following the excitation of nitromethane at 271 nm. A 406.5 nm laser pulse is used as the probe beam. Open circles are experimental measurements; solid lines are fits with a single exponential decay. Both transients show a fast decay ($\tau_D \approx 36$ fs) in the nπ^* excited electronic state of nitromethane. See text for further discussion.

the fragment ion mass peaks. The other possible mechanism for these TOFMS signals is that all the excited parent molecules are first ionized through resonance enhanced three-photon ionization and then some parent ions further dissociate into fragment ions within hundreds of nanoseconds inside the ionization region of the TOFM spectrometer. We call this an ionization−dissociation mechanism. In this later case, however, the line width for the fragment ion mass peaks will be broadened due to the fragmentation of nitromethane parent ion. Since the excess energy in the nitromethane parent ion is about 2 eV ($3 \times 4.57 - 11.08$ (IE) $= 2$ eV) after absorbing three photons at 271 nm, this is enough excess energy to open the three fragmentation channels to produce CH_3, NO_2, and NO ions directly from the parent ions.[55] The nitromethane parent ion mass peak has a line width of 10 ns, which is comparable to the instrumental line width of the TOFMS spectrometer, but the line width for the three fragment ion mass peaks in Figure 12 varies from 18 to 25 ns, which shows about 10 ns linewidth broadening for these fragment peaks. These broadened linewidths are evidence that the fragment ions are generated from fragmentation of the nitromethane parent ion, rather than from ionization of neutral dissociation products following $\pi^* \leftarrow$ n excitation of nitromethane. In combination with the nanosecond 271 nm pump−probe experiments, for which no NO_2, CH_3, CH_3O, or OH product signals are observed, we suggest that the ionization−dissociation mechanism is more probable for the production of the three fragments with only minor signal intensity. This mechanism is in good agreement with results reported by Kilics et al. for multiphoton ionization and dissociation of nitromethane using 375 nm femtosecond laser pulses.[55] The ionization−dissociation mechanism means that the nitromethane does not dissociate following $\pi^* \leftarrow$ n excitation at 271 nm in a supersonic molecular beam under collisionless conditions. This conclusion is in good agreement with Kwok et al.'s results that no dissociation products are observed after excitation of nitromethane at 266 nm under collision-free conditions.[36]

To confirm the validity of the proposed ionization-dissociation mechanism for the excitation of nitromethane at 271 nm, femtosecond pump−probe experiments are performed to measure the dynamics of the production of the three fragment ions. In this experiment, the pump beam at 271 nm is used to excite the parent molecule, and the probe beam at 406.5 nm is used to ionize the parent and fragments. The laser intensity of both pump and probe beams are kept low enough to reduce the ion signal by a factor of 100 produced by only a single beam. If nitromethane molecule dissociates into CH_3 and NO_2 after the excitation at 271 nm, the pump−probe transients for both CH_3 and NO_2 should present as a buildup near zero delay time, then reach a constant plateau after some longer delay time. On the contrary, if the nitromethane molecule does not dissociate at the nπ^* excited electronic state after 271 nm excitation, then we will see an ion signal enhancement for the nitromethane parent mass channel when both pump and probe beams are overlapped around zero delay time. Additionally, the lifetime of the excited state of nitromethane could be extracted from the pump−probe transient employing a single exponential decay function if it is long enough. Moreover, the fragment ion signal should have similar enhancement behavior around zero delay time since the fragment ion signal intensity is proportional to the parent ion signal intensity. In terms of energy for ionization, after excitation by a single photon at 271 nm, the nitromethane molecule needs another three photons at 406.5 nm to be ionized. The excess energy in the parent ion is about 2.6 eV ($1 \times 4.57 + 3 \times 3.05 - 11.08$ (IE) $= 2.64$ eV), which is also enough to open the three dissociation channels for the fragments. Figure 13 displays the pump−probe transients obtained by monitoring the nitromethane parent ion and CH_3 fragment ion mass channels. We do not observe a buildup around the zero delay time for the CH_3 fragment pump−probe transient, nor do we observe a constant plateau after a longer delay time. A signal enhancement when both pump and probe beams are overlapped is observed, however, which is similar to the pump−probe transient for the nitromethane parent ion. The transients for NO_2 and NO fragments are similar to those for the CH_3 fragment. This result further confirms that the fragment ions are produced from dissociation of the nitromethane parent ion. After deconvolution of the pump−probe transient of nitromethane parent ion by pump−probe pulse cross-correlation (τ_L=170 fs) and a single exponential decay, the decay time constant (τ_D) is determined to be 36 fs. Since the exponential signal decay is induced due to the depletion of the excited nπ^* state population

of nitromethane, we interpret the decay time constant to be the lifetime of the nπ^* state of nitromethane. To the best of our knowledge, this is the first time that the lifetime of the excited nπ^* state of nitromethane is determined. The ultrashort lifetime of the nπ^* state can well explain the broad absorption spectrum around the $\pi^* \leftarrow$ n transition of nitromethane. The reliability of the pump−probe measurement is confirmed by the duplication of the pump−probe transients for NO and NO_2 ions from the dissociative multiphoton ionization of NO_2 gas at around 400 nm, which has been reported by Eppink et al.[56] The pump−probe transients for both NO and NO_2 ions obtained in our measurements are comparable to those observed by Eppink and co-workers.

Both nanosecond and femtosecond 271 nm excitation of nitromethane show that dissociation of the nπ^* state of nitromethane does not occur even though the excitation energy at this wavelength is much larger than the dissociation energy (~2.6 eV) of the C−N bond. This result implies that the excited singlet state could undergo either intersystem crossing to a bound metastable triplet state with some vibrational excitation or internal conversion to the ground electronic state though conical intersections. Arenas and co-workers[57] have calculated that nitromethane could either dissociate into CH_3 and NO_2 at the nπ^* excited state or internally convert to the ground electronic state through two conical intersections following $\pi^* \leftarrow$ n excitation. Since no NO_2 dissociation product is observed in our experiments and the nπ^* state displays an ultrashort lifetime (36 fs), we suggest that nπ^* nitromethane returns to the ground electronic state by internal conversion though conical intersections. Intersystem crossing between singlet and triplet states is typically a slow process, but internal conversion through conical intersections could occur on the femtosecond time scale. Emission from the nπ^* state would also be quenched by this mechanism.

IV. Conclusions

After performing many experiments and careful analysis of the experimental data, we can integrate most of the existing photodissociation mechanisms for nitromethane following its two most intense absorption excitations, $\pi^* \leftarrow \pi$ and $\pi^* \leftarrow$ n. Our conclusions based on our own work and that of others are presented below.

Direct observation of intense CH_3, NO_2 (fs), and NO product signals from the photodissociation of nitromethane at 226 and 193 nm excitations confirms that the C−N bond rupture is the main primary process for the photolysis of nitromethane following the $\pi^* \leftarrow \pi$ excitation. Observations of OH and CH_3NO species with low quantum yield prove that OH formation and O atom elimination are minor channels for the dissociation of nitromethane after the $\pi^* \leftarrow \pi$ excitation. Formation of CH_3O radical after the dissociation of nitromethane at 226 and 193 nm excitation under only collisional conditions further confirms that the CH_3O radical is a result of the recombination of CH_3 and NO_2 products, and the nitro−nitrite isomerization does not occur for nitromethane following $\pi^* \leftarrow \pi$ excitation. Femtosecond pump−probe experiments at 226 nm show that the dynamics of the formation of CH_3 and NO_2, namely, the photodissociation dynamics of the nitromethane after the $\pi^* \leftarrow \pi$ excitation, is faster than our laser pulse duration (180 fs).

In nanosecond 271 nm laser experiments, a pump−probe scheme is employed to detect NO_2, CH_3, CH_3O, and OH products following the dissociation of nitromethane in the nπ^* excited electronic state; however, none of these fragments is observed. In femtosecond 271 nm laser experiments, nitromethane parent ion is observed with major intensity, together with three fragment ion signals (CH_3, NO_2, and NO) with only minor intensities. Pump−probe transients for both nitromethane parent and fragment ions at 271 nm excitation display a fast exponential decay with a time constant of 36 fs. We interpret this decay constant to be the lifetime of the excited nπ^* state of nitromethane. In combination with the 271 nm nanosecond pump−probe experiments, for which NO_2, CH_3, CH_3O, and OH fragment are not observed, we conclude that all the fragment ions generated in 271 nm femtosecond laser experiments are derived from the parent ion and dissociation of nitromethane from the nπ^* excited electronic state does not occur in a supersonic molecular beam under collisionless conditions.

Acknowledgment. This work is supported by a grant from the U.S. Army Research Office.

References and Notes

(1) Baly, E. C. C.; Desch, C. H. *J. Chem. Soc. London Trans.* **1908**, *93*, 1747.
(2) Purvis, J. E.; Mccleland, N. P. *J. Chem. Soc. Trans.* **1913**, *103*, 1088.
(3) Hantzsch, A.; Voigt, K. *Ber. Deutsch. Chem. Ges.* **1912**, *45*, 85.
(4) Zelinsky, N.; Rosanoff, M. A. *Z. Physik. Chem.* **1912**, *78*, 629.
(5) Thompson, H. W.; Purkis, C. H. *Trans. Faraday Soc.* **1936**, *32*, 674.
(6) Hirschlaff, E.; Norrish, R. G. W. *J. Chem. Soc.* **1936**, 1580.
(7) Kortum, G. Z. *Physik. Chem.* **1939**, *B43*, 271.
(8) Haszeldine, R. N. *J. Chem. Soc.* **1953**, 2525.
(9) De Maine, P. A. D.; De Maine, M. M.; Goble, A. G. *Trans. Faraday Soc.* **1957**, *53*, 427.
(10) Loos, Karl, R.; Wild, Urs, P.; Gunthard, Hans, H. *Spectrochim. Acta A* **1969**, *25*, 275.
(11) Nagakura, S. *Mol. Phys.* **1960**, *3*, 152.
(12) Bayliss, N. S.; McRae, E. G. *J. Phys. Chem.* **1954**, *58*, 1006.
(13) McAllister, T. *J. Chem. Phys.* **1972**, *57*, 3353.
(14) Flicker, W. M.; Mosher, O. A.; Kuppermann, A. *J. Chem. Phys.* **1980**, *72*, 2788.
(15) Rabalais, J. W. *J. Chem. Phys.* **1972**, *57*, 960.
(16) Chtistie, M. I.; Gillbert, C.; Voisey, M. A. *J. Chem. Soc.* **1964**, 3147.
(17) Brown, H. W.; Pimentel, G. C. *J. Chem. Phys.* **1958**, *29*, 883.
(18) Wodtke, A. M.; Hinsta, E. J.; Lee, Y. T. *J. Chem. Phys.* **1986**, *84*, 1044.
(19) Cundall, R. B.; Locke, A. W.; Street, G. C. *The Chemistry of Ionization and Excitation*; Johnson, G. R. A., Scholes, G., Eds.; Taylor and Francis Ltd.: London, 1967.
(20) Park, M. S.; Jung, K.-H.; Upadhyaya, H. P.; Volpp, H.-R. *Chem. Phys.* **2001**, *270*, 133.
(21) Zabarnic, S.; Fleming, J. W.; Baronavski, A. P. *J. Chem. Phys.* **1986**, *85*, 3395.
(22) Greenblatt, G. D.; Zuckermann, H.; Haas, Y. *Chem. Phys. Lett.* **1987**, *134*, 593.
(23) Rebbet, R. E.; Slagg, N. *Bull. Soc. Chim. Belges.* **1962**, *71*, 709.
(24) Gray, P.; Yoffe, A. D.; Roselaar, L. *Trans. Faraday Soc.* **1955**, *51*, 1489.
(25) Nicholson, A. J. C. *Nature* **1961**, *190*, 143.
(26) Avouris, P.; Chan, I. Y.; Loy, M. M. T. *J. Photochem.* **1980**, *13*, 13.
(27) Rockney, B. H.; Grant, E. R. *Chem. Phys. Lett.* **1981**, *79*, 15.
(28) McGarvey, J. J.; McGrath, W. D. *Trans. Faraday Soc.* **1964**, *60*, 2196.
(29) Napier, I. M.; Norrish, R. G. W. *Proc. R. Soc., Ser. A* **1967**, *299*, 317.
(30) Honda, K.; Mikuni, H.; Takahasi, M. *Bull. Chem. Soc. Jpn.* **1972**, *45*, 3534.
(31) Bielski, B. H. J.; Timmons, R. B. *J. Phys. Chem.* **1964**, *68*, 347.
(32) Colles, M. J.; Angus, A. M.; Marinero, E. E. *Nature* **1976**, *262*, 681.
(33) Spears, K. G.; Brugge, S. P. *Chem. Phys. Lett.* **1978**, *54*, 373.
(34) Schoen, P. E.; Marrone, M. J.; Schnur, J. M.; Goldberg, L. S. *Chem. Phys. Lett.* **1982**, *90*, 272.
(35) Mialocq, J. C.; Stephenson, J. C. *Chem. Phys.* **1986**, *106*, 281.
(36) Kwok, H. S.; He, G. Z.; Sparks, R. K.; Lee, Y. T. *Int. J. Chem. Kinet.* **1981**, *13*, 1125.
(37) Blais, N. C. *J. Chem. Phys.* **1983**, *79*, 1723.

(38) Butler, L. J.; Krajnovich, D.; Lee, Y. T. *J. Chem. Phys.* **1983**, *79*, 1708.
(39) Moss, D. B.; Trentelman, K. A.; Houston, P. L. *J. Chem. Phys.* **1992**, *96*, 237.
(40) Lao, K. Q.; Jensen, E.; Kash, P. W.; Butler, L. J. *J. Chem. Phys.* **1990**, *93*, 3958.
(41) Arenas, J. F.; Otero, J. C.; Pelaez, D.; Soto, J. *J. Chem. Phys.* **2003**, *119*, 7814.
(42) Im, H. -S.; Bernstein, E. R. *J. Chem. Phys.* **2000**, *113*, 7911.
(43) Guo, Y. Q.; Greenfield, M.; Bernstein, E. R. *J. Chem. Phys.* **2005**, *122*, 244310.
(44) Greenfield, M.; Guo, Y. Q.; Bernstein, E. R. *Chem. Phys. Lett.* **2006**, *430*, 277.
(45) Guo, Y. Q.; Greenfield, M.; Bhattacharya, A.; Bernstein, E. R. *J. Chem. Phys.* **2007**, *127*, 154301.
(46) Trebino, R. *Frequency-Resolved Optical Grating: The Measurement of Ultrafast Laser Pulses*; Kluwer Academic Publisher: Boston, 2000.
(47) Hippler, M.; Pfab, J. *Chem. Phys. Lett.* **1995**, *243*, 500.
(48) Herzberg, G. *Molecular spectra and molecular structure, Vol. 1. Spectra of Diatomic Molecules*; Van Nostrand, NY, 1950.
(49) Ahmed, M.; Peterka, D. S.; Suits, A. G. *Atomic and Molecular Beams*; Campargue, R., Ed.; Springer-Verlag: Berlin, Germany, 2001.
(50) Herzberg, G. *Molecular spectra and molecular structure, Vol. 3. Electronic spectra and electronic structure of polyatomic molecules*; Kreiger, Malabar, 1988.
(51) Im, H.-S.; Bernstein, E. R. *J. Phys. Chem. A* **2002**, *106*, 7565.
(52) Mijoule, C.; Odiot, S.; Fliszar, S.; Schnur, J. M. *J. Mol. Struct.* **1987**, *149*, 311.
(53) Johnson, H; Graham, R. *J. Phys. Chem.* **1973**, *77*, 62.
(54) Jacobs, A; Kleinermanns, K; Kuge, H; Wolfrum, J. *J. Chem. Phys.* **1983**, *79*, 3162.
(55) Kilic, H. S.; Ledingham, K. W. D.; Kosmidis, C.; McCanny, T.; Singhal, R. P.; Wang, S. L.; Smith, D. J.; Langley, A. J.; Shaikh, W. *J. Phys. Chem. A* **1997**, *101*, 817.
(56) Eppink, A. T. J. B.; Whitaker, B. J.; Gloaguen, E.; Soep, B.; Coroiu, A. M.; Parker, D. H. *J. Chem. Phys.* **2004**, *121*, 7776.
(57) Arenas, J; Otero, J; Pelaez, D; Soto, J. *J. Chem. Phys.* **2005**, *122*, 084234.

JP806230P